Low Molecular Weight Inhibitors of the Protease Anthrax Lethal Factor

Georgios A. Dalkas[1], Athanasios Papakyriakou[1], Alexios Vlamis-Gardikas[2] and Georgios A. Spyroulias[1,*]

[1]*Department of Pharmacy, University of Patras, Panepistimioupoli - Rion, GR-26504, Patras, Greece;* [2]*Department of Biochemistry, Biomedical Research Foundation (BRFAA), Academy of Athens, Soranou Effesiou 4, GR-11527, Athens, Greece*

Abstract: Anthrax Lethal Factor (LF) is a zinc-dependent metalloprotease that together with the protective antigen constitute the anthrax lethal toxin, the most prominent virulence factor of the disease anthrax. This review summarizes the current knowledge on anthrax toxicity and defense in relation to LF. Particular emphasis is placed on the structural aspects of LF, the properties of its substrates and the achievements in the design of low molecular weight inhibitors of the catalytic activity of the metalloenzyme.

Key Words: Anthrax lethal factor (LF), mitogen-activated protein kinase kinase (MAPKK), small molecular weight inhibitors, structure-based drug discovery, zinc-metalloprotease.

INTRODUCTION

Anthrax, the infectious disease of animals and humans caused by the gram-positive bacterium *Bacillus anthracis* (*B. anthracis*), has been a notorious disease since antiquity. Recently it has attracted the interest of many academic laboratories in view of its potential use as a biological weapon. An anthrax attack with spores delivered by aerosol could cause inhalation anthrax, an extraordinarily rare and deadly form of the naturally occurring disease. The spores can survive in the ground for long periods. Anthrax occurs when *B. anthracis* endospores enter the body through abrasions in the skin or by inhalation or ingestion. While cutaneous anthrax is rarely lethal, the inhalation of the spores is often fatal. The most common cutaneous form is initially manifested as a small pimple that develops within a few days, into black skin lesions. Hence the origin of the name "Anthrax", derived from the Greek words *anthrax*, *anthrakis* for coal, in reference to the black eschar characteristics observed on the skin of infected individuals. The skin form is easily diagnosed and can be treated with a variety of antibiotics. In gastrointestinal and inhalational forms, the illness is insidious at first, with mild symptoms of gastroenteritis, slight fever, and flu-like symptoms. Early diagnosis is difficult. The disease may abruptly develop into a systemic form irresponsive to treatment, leading to death; systemic infection resulting from inhalation of the organism has a highly mortality rate, with death usually occurring within 48 h afther the onset of symptoms [1-6].

PATHOGENESIS

Inhalational anthrax begins after the uptake of spores by pulmonary macrophages that carry the spores to regional lymph nodes, while the spores germinate *en route*. Anthrax bacilli multiply in the lymph nodes, and spread throughout the body in the bloodstream, where they live as extracellular pathogens to reach high numbers (until there are as many as 10^7 to 10^8 organisms per milliliter of blood), causing massive septicemia and toxemia that has systemic effects that can lead to death of the host [2].

The major virulence factors of *B. anthracis* are encoded on plasmids, pXO1 and pXO2. Plasmid pXO1 (184.5 kb) carries the genes *cya* (coding for edema factor; EF), *lef* (encoding lethal factor; LF) and *pagA* (coding for protective antigen; PA). The three genes contribute in the formation of the two secreted anthrax toxins [1-6]. Plasmid pXO2 (95.3 kb) contains the genes (*capB*, *capC*, and *capA*) involved in the synthesis of the poly-D-glutamic capsule that normally surrounds the bacterium.

The anthrax to the xins represent a variation on the A-B model, characteristic of a number of well-studied toxins. The general principle is that the B (binding) moiety attaches the toxin to the target cell to facilitate entry of the A (catalytic or effector) part into the cytoplasm [7]. The B part in both anthrax toxins is represented by PA, a single receptor of 83 kDa. The A part can be either EF (89 kDa), giving with PA the edema toxin (ETx = EF-PA) or LF (90 kDa), generating with PA the lethal toxin (LTx = LF-PA). EF is a calmodulin-dependent adenylate cyclase that increases intracellurar levels of cyclic AMP (cAMP) on entry into most types of cells. LF is a zinc-dependent metalloprotease with high specificity to the family of mitogen-activated protein kinase kinases (MAPKKs), cleaving them near to their amino termini. ETx is considered responsible for phagocyte inhibition and the massive edema that is manifested in anthrax infection. LTx is the major cause of death of infected organisms. The unique poly-D-glutamic capsule of *B. anthracis* inhibits phagocytosis of vegetative cells. Both pXO plasmids are required for full virulence; the loss of either one results in an attenuated strain [1-6].

Expression of the toxin and capsule genes by *B. anthracis* during *in vitro* growth is influenced by culture condi-

*Address correspondence to this author at the Department of Pharmacy, University of Patras, Panepistimioupoli – Rion, GR-26504, Patras, Greece; Tel: +30 2610 969950 (office), -951 & 952 (lab); Fax: +30 2610 969 950; E-mail: G.A.Spyroulias@upatras.gr

1389-5575/08 $55.00+.00

tions. Capsule and toxin expression is enhanced during growth in certain minimal media in the presence of bicarbonate or under elevated (5% or greater) atmospheric CO_2. In addition, toxin synthesis is increased during growth at 37°C as compared to 28°C. Two genes have been identified as *trans*-acting regulators of toxin and capsule gene transcription. The pXO1-encoded gene *atxA* (anthrax toxin activator) activates transcription of all three toxin genes. The pXO2-encoded gene *acpA* activates transcription of *capB* [8-12].

ACTION OF THE ANTHRAX TOXINS

Cellular toxicity begins when PA [13] binds on to the membrane-bound surface-exposed anthrax toxin receptor ATR (Fig. **1**). The latter is a type I membrane protein with an extracellular von Willebrand factor A domain [14]. Following binding, a furin-like cell-surface membrane protease activates PA by cleaving its N-terminal 20 kDa fragment (PA_{20}) in the extracellular milieu to generate the mature 63-kDa C-terminal fragment (PA_{63}) [15]. The released PA_{20} diffuses away, and plays no further part in toxin action. The PA_{63} fragment oligomerizes to form symmetric, ring-shaped, membrane-inserting heptamers, $[PA_{63}]_7$, capable of binding up to three molecules of either edema factor or lethal factor [16]. The entire complex is then trafficked to the endosome, where the low-pH environment induces the PA_{63} pre-pore structure to insert into the membrane and form the channel through which EF and LF pass to the cytosol. Once there, EF and LF carry out their respective damage-inducing processes.

EF acts as a Ca^{2+}/calmodulin-dependent adenylate cyclase to greatly elevate the intracellular levels of cAMP. This is a strategy employed by many other bacteria, resulting in disarray of the intracellular signaling pathways. The increase in cATP hampers the oxidative burst and pro-inflammatory cytokine expression and migration of polymorphonuclear cells and macrophages, allowing thus bacteria to evade the immune system [17]. In addition, LF kills directly the macrophages: once intracellular, LF acts as a Zn^{2+}-dependent endoprotease that cleaves members of MAPKKs at their N-termini, disrupting their ability to interact with and phosphorylate downstream substrates [18,19]. The overall effect is altered signaling pathways and ultimately apoptosis where macrophages lyse *via* a mechanism not entirely understood [20]. Thus, PA with EF or LF (anthrax toxins) may act in synergy to enter the cell and disrupt cellular function, leading ultimately to cell death.

MITOGEN-ACTIVATED PROTEIN KINASE KINASES

The MAPKK family is comprised of seven members; two MEKs [MAPK/ERK (extracellular-signal-regulated kinase) kinase] 1 and 2 (MEK1, MEK2) and five MKKs [MAPK (mitogen-activated protein kinase) kinases] MKK3, MKK4, MKK5, MKK6 and MKK7. The MAPKKs MEK1 and MEK2 specifically phosphorylate and activate the ERK1 and ERK2 MAPKs. MKK3 and MKK6 are specific for the MAP kinase $p38^{hog}$, whereas MKK4 and MKK7 phosphoactivate the stress-activated protein kinase JNK (c-Jun N-terminal kinase), although MKK4 can phosphorylate $p38^{hog}$ as well [21-23]. MEK5 is the most distant member of the family and is known to phosphoactivate MAPK $Bmk1/ERK5^{MAPK}$.

Cleavage occurs within a stretch of amino acids of the loose consensus ++++X*h*X↓*h* (basic and hydrophobic residues are indicated by + and *h* respectively, X indicates any amino acid while the cleavage site is indicated by ↓) (Table **1**). The active site of the protease is divided in different subsites that may come into contact with the substrate. The subsites interacting with the N-terminus of the substrate are numbered S1–Sn (non-primed sites), while those that interact with the C-terminus are numbered as S1'–Sn' (primed sites). The numbering begins from the sites located on each side of the scissile bond. The corresponding substrate residues that the protease subsites interact with are numbered P1–Pn, and P1'–Pn', respectively [24]. Alignment of the substrate regions centered at their cleavage sites shows that position P1′ is always occupied by a hydrophobic residue, as is position P2, apart from MEK1 (Table **1**). Moreover, one or more posi-

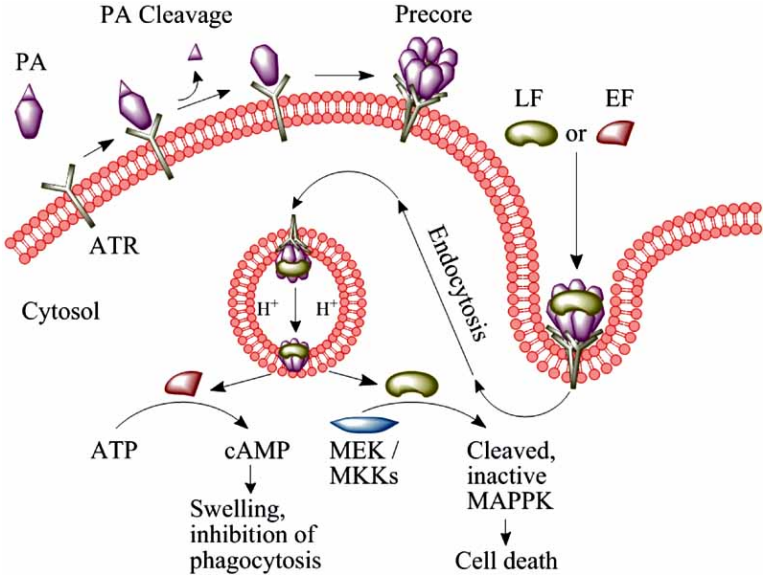

Fig. 1. A schematic representation of cell entry of the anthrax toxins.

Table 1. Known LF Cleavage Sites in Mammalian MKKs (Underlined). Conserved Residues are in Bold and Marked as (+) for Basic, (h) for Hydrophobic. (X) Indicates any Amino Acid

Substrate	LF Cleavage Site															
	P8	**P7**	**P6**	**P5**	**P4**	**P3**	**P2**	**P1**	**P1′**	**P2′**	**P3′**	**P4′**	**P5′**	**P6′**	**P7′**	**P8′**
MEK1$_{(1-16)}$	M	P	K	K	K	P	T	P	I	Q	L	N	P	A	P	D
MEK2$_{(3-18)}$	A	R	R	K	P	V	L	P	A	L	T	I	N	P	T	I
MKK3b$_{(19-34)}$	S	K	R	K	K	D	L	R	I	S	C	M	S	K	P	P
MKK6b$_{(7-22)}$	K	K	R	N	P	G	L	K	I	P	K	E	A	F	E	Q
MKK4$_{(38-53)}$	Q	G	K	R	K	A	L	K	L	N	F	A	N	P	P	F
MKK4$_{(51-66)}$	P	P	F	K	S	T	A	R	F	T	L	N	P	N	P	T
MKK7β$_{(37-52)}$	P	R	P	R	P	T	L	Q	L	P	L	A	N	D	G	G
MKK7β$_{(69-84)}$	A	R	P	R	H	M	L	G	L	P	S	T	L	F	T	P
Consensus		+	+	+	+	X	h	X	h							

tively charged residues are present between positions P4 and P8, suggesting that electrostatic interactions are also necessary for a correct positioning of the substrate within the active site of LF. The active site of LF is acidic and nicely complements the basic residues at multiple positions of the N-termini of the six MAPKKs substrates. Table **1** shows all known cleavage sites of mammalian MAPKKs. LF cleaves MEK1, MEK2, MKK3 and MKK6 once, while MKK4 and MKK7 are cleaved twice [21,22].

INVESTIGATION OF THE SEQUENCE AND STRUCTURE OF LF

The crystallographic structure of LF shows that the molecule is organised in four domains rich in α-helices [25] (Fig. **2A**). The active site is a broad deep groove, 40 Å long. It is created by the vestigial NAD-binding pocket of domain II and by the interface between domains II, III and IV. The groove has in general a negative potential, containing clusters of glutamic acid/aspartic acid, as well as glutamine/asparagine residues [25]. The N-terminal domain (residues 1–262, Domain I) is responsible for binding to PA. The region comprising residues 263-297 and 385-550 (Domain II) exhibits a remarkable structural similarity to the catalytic domain of the *B. cereus* toxin, VIP2. However, a critical glutamic acid that is conserved throughout the family of ADP ribosylating toxins is replaced by a lysine (K518), which probably abolishes any ADP-ribosylating activity. Domain III comprises residues 303–382 that shape the boundary of the cleft-shaped active site of LF and is required for enzymatic activity; insertional mutagenesis and point mutations in this domain abrogate LF's activity [26]. It makes limited contact with domain II, but shares a hydrophobic surface with domain IV. Domain III provides steric hindrance to severely restrict access to the active site (located in domain IV) of potential substrates, for example loops of globular proteins. On the other hand it could accommodate a flexible 'tail' from a protein substrate. It also attributes sequence specificity to LF by making specific interactions with substrates.

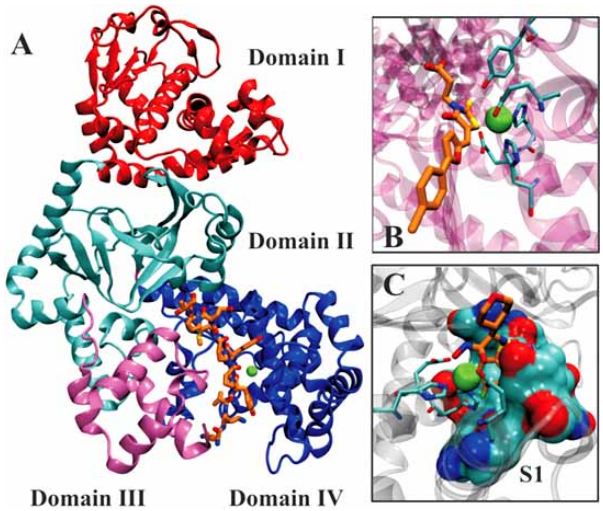

Fig. 2. (A) Ribbon representation of the X-ray crystal structure of the LF–MAPKK2 complex (PDB ID: 1JKY). The substrate is depicted as stick model, and the zinc ion as green sphere. **(B)** Crystal structure of the LF–BI-MFM3 complex (compound **62**, PDB ID: 1ZXV) showing the zinc-coordinating residues (His686, Glu735, His690), the catalytic residues (Glu687, Tyr728) and the inhibitor in stick representation. **(C)** Crystal structure of LF in complex with LF inhibitor (compound **39**, PDB ID: 1YQY) showing the S1′ pocket as a surface representation. Figures were rendered using the program VMD 1.8.5 [27].

Domain IV formed by amino acids 552–776 is the heart of the proteolytic activity of LF. It contains the two Zn-binding motif sequences ($H_{686}E_{687}F_{688}G_{689}H_{690}$ and $E_{735}F_{736}F_{737}A_{738}E_{739}$) that bind to zinc with a stoichiometry of 1:1. The two sequences are separated by a spacer of 44 residues (Fig. **2B**, **C**) [28]. The active site zinc ion is coordinated tetrahedrally by a water molecule and the three side chains of His686, His690, and Glu735. Mutation of the active site residues within the first coordination shell around the zinc, partially or totally impaired LF activity [29,30]. Such coor-

dination resembles that of the thermolysin family of metalloproteases. However, analysis of the second shell of residues surrounding the zinc ion (within 5 Å) revealed the presence of a tyrosine residue (Tyr728) that is also present in thermolysin. A similar tyrosine is instead present in the clostridial metalloprotease neurotoxins that comprises eight members: seven botulinum neurotoxins and one tetanus neurotoxin. Mutation of this tyrosine of tetanus neurotoxin (Tyr-375) and in botulinum neurotoxin type A (Tyr-366) into an alanine impairs their proteolytic activity, suggesting that the phenolic side chain plays a role in catalysis and/or in substrate binding [30]. Glu687 acts as a general base to activate the zinc-bound water molecule during catalysis and Tyr728 (located on the opposite side of Glu687) has been previously proposed to function as a general acid to protonate the leaving amino group [30]. With respect to its Zn-binding site, LF is classified in the MA clan and M34 family of Zn-metalloproteases [31], where the two histidines of the HEXXH motif (X is any amino acid) are ligands of the zinc ion, while the glutamate participates in catalysis.

LF INHIBITORS (LFis)

LF is central in anthrax toxicity. The fact that EF-deficient *B. anthracis* strains are still toxic, while those lacking LF are greatly attenuated, suggests that LF is the dominant virulence factor of anthrax. Therefore, the inhibition of LF proteolytic activity is a promising method for treating exposure to *B. anthracis* spores [32]. Several groups have reported the use of *in vitro* protease assays to identify LF inhibitors (LFis) that in some cases were further analyzed in cell-based assays.

1. Hydroxamate-Based Inhibitors

The first LFis were peptide hydroxamates designed on the basis of the N-terminal sequence of MEKs, with the addition of a cluster of positive charges to increase cell penetration [33-35]. Investigation of the inhibition of LF by hydroxylamine derivatives *in vitro*, identified compounds with nanomolar inhibition constants. In particular the competitive inhibitor In-2-LF (AcGYβARRRRRRRRVLR-hydroxamate, compound **1**, Table **2**), had a K_i of 1 nM [33]. By incorporating a metal-chelating moiety in various peptide substrates, the potent inhibitor MKARRKKVYP–NHOH (K_i = 0.0011 μM) was generated (compound **2**, Table **2**) [34,35]. Using this information, additional peptidic inhibitors were identified [35]. Remarkable inhibition was reported for a small compound containing primed side residues, 2-thioacetyl-YPM-amide (SHAc-YPM, compound **3**, Table **2**). The compound comprises a N-terminal metal chelating group followed by a hydrophobic residue at the P1' position, an arrangement shared by compounds previously reported to inhibit matrix metallo-proteinases (MMPs) [35-37]. In the crystal structure of the LF-SHAc-YPM complex (PDB ID: 1PWQ) [35], the carbonyl oxygen atom and the thiol sulphur atom of the thioacetyl moiety are directed toward the zinc, while the P1' tyrosine is buried in the S1′ pocket. Further searches for LFis among other known matrix metalloprotease inhibitors identified a 2 μM competitive inhibitor, GM6001 (compound **4**, Table **2**), (3-(N-hydroxycarboxamido)-2-isobutyl-propanoyl- Trp-methylamide), that is an N-terminal hydroxamic acid with a P1' leucine-mimetic, a P2' tryptophan and a C-terminal methyl group [35,38]. The crystal structure of the LF (E687C mutant)-GM6001 complex (PDB ID: 1PWU) shows that the planar hydroxamate moiety is directed toward the zinc. The leucine-mimetic side chain is accommodated in the S1′ pocket, interacting with the hydrophobic residues Val675 and Leu677, while the P2' tryptophan side chain makes no specific contacts with the protein. GM6001 provided high protection from death even when added to cell cultures three hours after addition of LF, sug-

Table 2. Hydroxamate-Based Inhibitors

Compound	LF Inhibitor Chemical Structure	K_i (nM)
1	**AcGYβARRRRRRRRVLR-hydroxamate (In-2-LF)**	1
2	**MKARRKKVYP–NHOH**	1
3	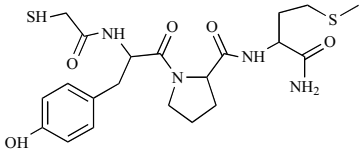 **2-thiolacetyl-YPM-amide**	11,000
4	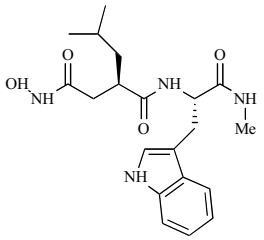 **GM 6001**	2,000

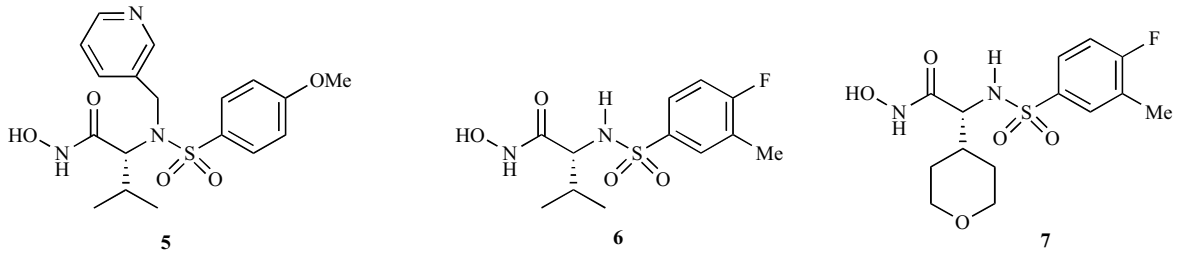

5 **6** **7**

Scheme 1.

gesting it could protect cells even after internalization of LTx [35].

More hydroxamate-based inhibitors were identified among already known matrix metalloproteinase inhibitors, the rational being that LF itself is a metalloproteinase [39,40]. Large chemical libraries of small-molecule MMPis comprised mainly of hydroxamate-, carboxylate- and sulfhydryl-based molecules capable of chelating the active site Zn(II) ion [41]. Three broad-spectrum MMPis that are in the early stages of development as pharmaceuticals, CMT-300, CMT-308 and Ilomastat (GM6001) (compound **4**, Table **2**), were effective competitive inhibitors of LF [42] with apparent K_i values of less than 7 μM. Moreover, all three LFis could inhibit LF in viable cells when employed prior to addition of LF and PA according to the "preexposure prophylaxis" protocol (U.S. Food and Drug Administration).

2. Zinc Metalloprotease-Based Inhibitors

Researchers at Merck Laboratories and collaborators utilized targeted screening of known Zn-metalloprotease inhibitors and identified compound **5** (Scheme **1**), a low micromolar LFi (12 μM IC_{50}) [43]. IC_{50} is a parameter used in pharmacological research. IC_{50}, the half maximal inhibitory concentration, represents the concentration of an inhibitor that is required for 50% inhibition of its target (i.e. an enzyme, cell, cell receptor or a microorganism). By systematically changing various parts of compound **5**, they synthesized compound **6** (Scheme **1**) with an IC_{50} value of 0.13 μM. Shoop *et al*. described a time-dependent, reversible LFi with an IC_{50} value of 54 nM (compound **7** in Scheme **1**) [44]. The kinetic mechanism of inhibition for LFi was determined to be competitive with the substrate, with a K_i value of 24 nM. The crystal structure analysis of the complex (PDB ID: 1YQY) revealed that the inhibitor was located in the catalytic domain at the interface of domains III and IV with the 4-fluoro-3-methylphenyl group optimally filling the deep S1′ hydrophobic pocket (Fig. **2**) [44]. In addition, the inhibitor exhibited 100% protection in a lethal mouse toxemia model against recombinant PA and LF, and gave 100% protection when administered in combination with ciprofloxacin in a rabbit model of active *B. anthracis* infection [44]. Due to its good water solubility, excellent selectivity profile against MMPs and a wide array of enzyme or receptor targets, the inhibitor was selected as a candidate for clinical studies and drug development [44].

3. Aminoglycoside-Based Inhibitors 1: Neomycin B

To identify novel LFis, Wong and co-workers utilized a library of approximately 3000 compounds that was screened in a 96-well fluorescent assay format [45]. Several known and novel synthetic aminoglycosides were tested in secondary rounds of screening. The K_i values of the aminoglycosides with the highest inhibitory activities are shown in Table **3** (compounds **8**-**11**). Neomycin B, a commonly utilized antibiotic of the aminoglycoside family, emerged as the most potent inhibitor of LF (compound **11**, Table **3**) [45]. These aminoglycosides were competitive inhibitors of LF.

The interaction of neomycin B with bacterial rRNA and LF is mainly determined by electrostatic interactions [46]. It

Table 3. Structures of Synthetic Aminoglycoside Dimers

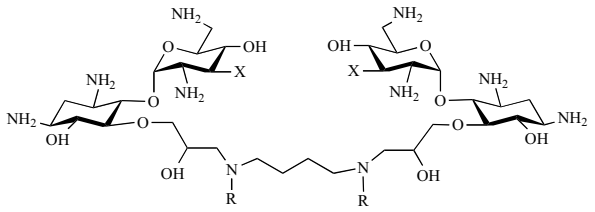

Compound	X	R	K_i (nM)
8	OH	CH_3	14.1
9	OH	H	14.4
10	H	H	28.5
11	Neomycin B		7.0

was postulated that superior binding to both rRNA and LF, resulting in dual- anti-anthrax effect, could occur after adding recognition and binding elements to neomycin B [46]. The improved antibacterial activity of the first generation of pseudopentasaccharide derivatives of neomycin B (compound **11**, Table **4**), compounds **12**–**15** (Table **4**) [47], along with the inhibition of various nucleic acid metabolizing enzymes by aminoglycosides [48], support this hypothesis. Taking into consideration the relative ease of derivatizing a primary alcohol, position C5" in neomycin B was selected for modification and a new series of derivatives was generated (compounds **16**–**23**, Table **4**). Using an *in vitro* fluorescence assay, compounds **12**–**23** were all competitive inhibitors of LF protease activity (Table **4**) [46]. Under low-ionic-strength assay conditions, 6 compounds (**13**, **17**, **20**–**23**) of the 12 analogues tested had K_i values in the range of 0.2–1.3 nM, proving thus significantly better inhibitors than neomycin B itself (K_i=37 nM).

Table 4. Structures of Neomycin B and the Synthetic Analogues

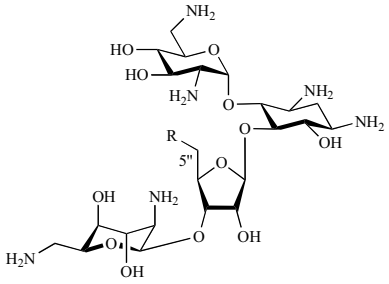

Compound	R	K_i (nM) low / high [salt]
11 (Neomycin B)	–OH	37 / 59
12	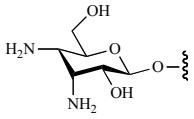	11 / 50
13	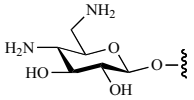	0.5 / 28
14	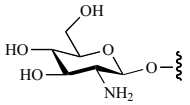	13 / 66
15	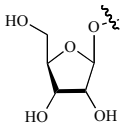	28 / 134
16	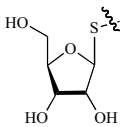	52 / 81
17	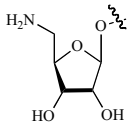	1.3 / 3.9
18	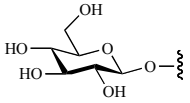	23 / 125

(Table 4. Contd….)

Compound	R	K_i (nM) low / high [salt]
19	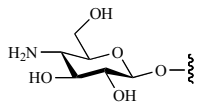	15 / 85
20	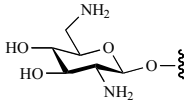	0.6 / 20
21	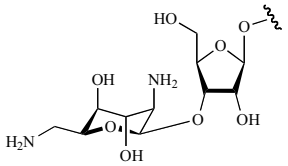	0.4 / 21
22	–SH	0.2 / 10
23	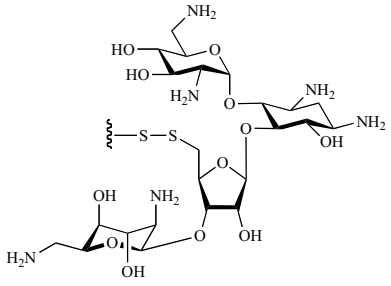	0.7 / 1.1

4. Aminoglycoside-Based Inhibitors 2: Neamine

As the structural complexity of neomycin B renders it unattractive for drug discovery, Jiao *et al*. [49] focused on the simpler compound neamine (compound **24**, Scheme **2**), the core structure of neomycin B. Neamine was a weak inhibitor of LF (K_i=42.9 μM) [49]. To improve the potency of neamine, a library of selectively guanidinylated analogs was synthesized (Scheme **2**) with mono-, di-, and tri-guanidinylated derivatives of neamine [50]. These molecules proved potent, selective inhibitors of LF with K_i between 0.5 and 24.3 μM [49]. Among them, 1,3,2′,6′-tetraguanidinoneamine (compound **34**), 1,3,2′-triguanidinoneamine (compound **35**) and 3,2′-diguanidinoneamine (compound **36**) exhibited the most potent activities in the sub-micromolar range (Table **5**). A by-product of the research for neamine analogues [51] was the the non related polyamine spermine that could also inhibit LF (K_i of 0.9 ± 0.09 μM) [51].

5. Aminoglycoside-Based Inhibitors 3: 2,5-Dideoxystreptamine Derivatives

Despite their good *in vitro* performance, the use of guanidinylated neamine analogs as anti-anthrax drugs seems an unattainable goal due to their poor oral bioavailability and potential toxicity. To avoid the undesirable pharmacological profile of neamine and maintain a similar inhibition against LF, easily accessible mimetics of guanidinylated neamines were tested. To simplify analog synthesis, the related core structure 2,5-dideoxystreptamine that preserves the same unique spatial arrangement of the amino-groups of 2-deoxystreptamine (itself a part of neomycin B [49]), was used. Since the presence of guanidinyl groups in neamine analogs was indispensable for their potency, similar replacement of the amino sugar with a guanidinylated aryl ring seemed plausible. It was assumed that these planar non-sugar groups would increase the lipophilicity and bioavailability of the

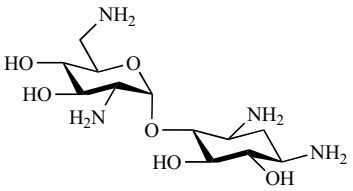

24

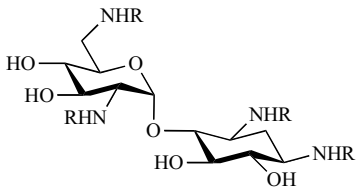

neamine analogs

Scheme 2.

Table 5. Structures of Guanidinylated 2,5-Dideoxystreptamine Aryl Ethers

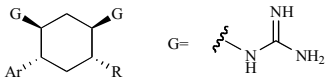

Compound	Ar	R	K_i (μM)
25	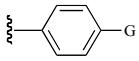	OH	14.9
26		OH	30.6
27	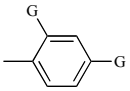	OH	0.6
28	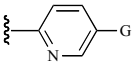	OH	6.6
29	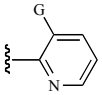	OH	4.1
30	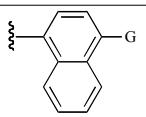	OH	31.4
31	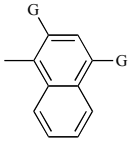	OH	10.7
32	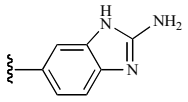	OH	153.7
33	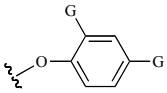	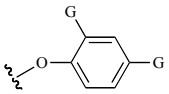	0.065
34	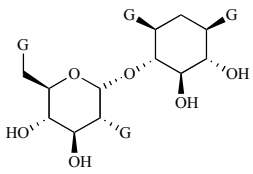		0.7
35	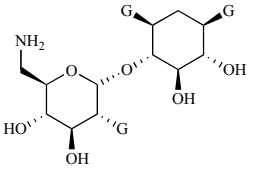		0.5

(Table 5. Contd….)

Compound	Ar	R	K_i (μM)
36	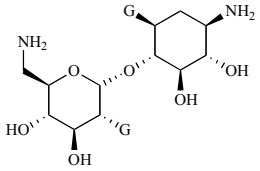		0.7

compound [49]. The guanidinylated 2,5-dideoxystreptamine aryl ethers (Table **5**) were selected as the initial target compounds. While the corresponding amino-precursors showed very weak or no activity against LF, the guanidinylated 2,5-dideoxystreptamine derivatives were potent inhibitors (Table **5)**. The more guanidinyl groups present, the better the activity observed (compounds **27** *vs* **25** and **26**, and **31** *vs* **30**) [49]. Generation of the symmetric meso-compound **33** by replacing each of the free 6-OH groups with a 2,4-diguanidino-phenoxy moiety gave inhibition in the nano-molar range [49].

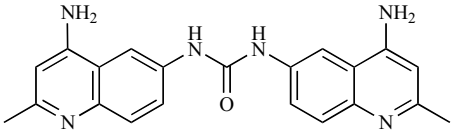

37

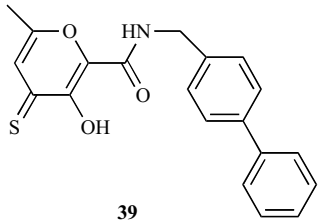

39

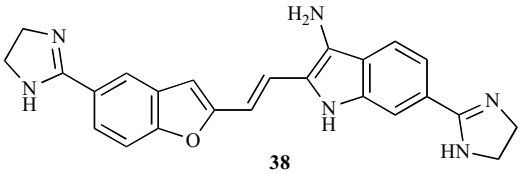

38

Scheme 3.

6. N,N′-di-Quinoline Urea Derivatives

The National Cancer Institute's (NCI's) Diversity Set was analysed using a high-throughput assay [52]. Two competitive inhibitors, NSC12155 and NSC357756 were identified with K_i values of 0.5 and 4.9 μM respectively (compounds **37** and **38**, Scheme **3**). NSC12155 is a N,N′-diquinoline urea derivative that binds to the active site of LF by positioning the urea moiety close to the zinc atom, with one quinoline near the side chain of His690. The X-ray crystal structure of the LF-NSC12155 complex solved at 2.9 Å resolution (PDB ID: 1PWP) revealed that the inhibitor bound to the catalytic site of LF with its urea moiety close to the catalytic zinc ion [52]. One quinoline ring was detected near the His690 ligand demonstrating π-stacking interactions while the other ring exhibited a preference for a "C-shaped" conformation. The conformational spaces of two leads, NSC12155 and NSC357756, were subsequently explored to generate multiple pharmacophoric hypotheses, used in 3D database mining studies to identify additional LFis [52]. Six additional LFis were identified, but none more effective than NSC12155. None of the inhibitors performed well in the *in vitro* cytotoxicity test on cultured macrophages, possibly due to lack of membrane permeability. As with the screening of the hydroxamate-based inhibitors described previously [35], results of animal tests were not reported [52,53].

7. Heterocyclic Zinc-Chelators

To overcome the limitations of hydroxamate-based inhibitors, Lewis *et al*. evaluated a number of heterocyclic zinc-binding groups against LF *in vitro* [54]: sulfur-containing ligands had lower IC_{50} values for LF. This is consistent with earlier findings regarding these ligands and their inhibitory effect on MMPs. By attaching a biphenyl backbone to a thiopyrone zinc-binding group, AM-2S was synthesized (compound **39**, Scheme **3**). The compound showed comparable inhibitory efficacy (14 μM IC_{50}) to other LFis [53].

8. Drug Structure Scaffolds

Pellecchia and co-workers [55] utilized an iterative approach in discovering a very potent LFi. An initial screening of ~300 compounds representing most of the drug structure scaffolds identified an inhibitor with an IC_{50} value of 140 μM (compound **40** in Table **6**). Based on this scaffold, 22 of its most representing derivatives were spotted at commercially available repositories and were tested by both NMR- and fluorescence-based assays (Table **6**). The most potent

Table 6. Phenylfuran-2-ylmethylenerhodanineacetic Acid Derivatives Tested Against LF

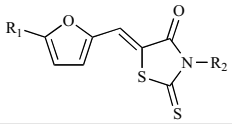

Compound	R_1	R_2	IC_{50} (μM)
40	H	$-CH_2COOH$	140
41	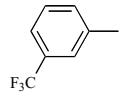	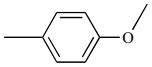	300
42	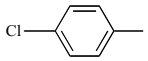	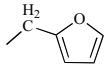	150
43	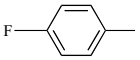	$-CH_2CH=CH_2$	50
44	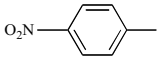	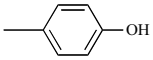	37.7
45	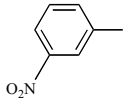	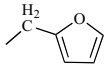	38.3
46	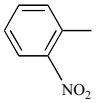	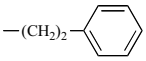	31.9
47	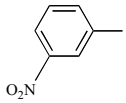	$-(CH_2)_3COOH$	20
48	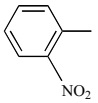	$-(CH_2)_2COOH$	12.8
49	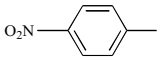	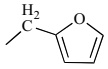	12.6
50	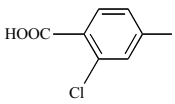	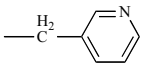	9.9
51	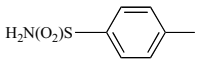	$-CH_2COOH$	9.1
52	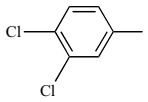	H	7.4
53	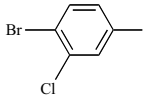	H	7.0
54	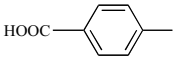	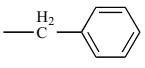	6.0

(Table 6. Contd….)

Compound	R_1	R_2	IC_{50} (μM)
55	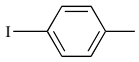	–CH_2COOH	5.5
56	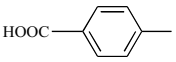	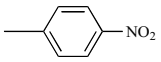	4.8
57	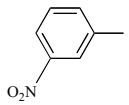	–CH_2COOH	3.1
58	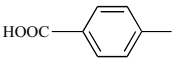	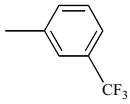	2.9
59	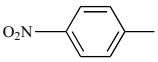	–$(CH_2)_2$COOH	2.7
60	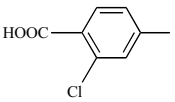	–CH_2CH=CH_2	2.7
61	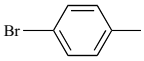	–$(CH_2)_3$COOH	2.3
62	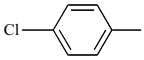	–$(CH_2)_2$COOH	0.8

(competitive) inhibitor, was compound **62** (Table **6**) with an IC_{50} of 1.7 μM. The compound **62** was very specific for LF as it did not inhibit MMP-2 and MMP-9 at concentrations up to 100 μM. Data from X-ray crystallography (PDB ID: 1ZXV) revealed the interaction of the rhodanine ring of compound **62** with zinc(II) *via* the thiazolidine sulfur atom. The carboxylic group pointed toward an hydrophilic region of the protein (Fig. **2B**). On the basis of the acquired structure-activity data, several analogues of compound **62** were synthesized and screened by both assays (Table **7**). Submicromolar activity LFis were identified with the most potent being compound **69** (K_i ~ 32 nM). Recently, the same group has reported further qualitative structure-activity relationship (QSAR) and comparative molecular field analysis (CoMFA) studies on newly derived inhibitors [56]. The resulting 3D QSAR model provides a basis for the rational design of novel LFis with improved activity and selectivity.

9. Hydrazone-Based Molecules

A hydrazone-based small molecule, (DS-998, compound **70**, Table **8**), was identified as a potent non-competitive LFi (K_i of 1.1 μM) using a novel *in vitro* assay [57]. Measurements of LF activity were performed directly by MALDI-TOF on LF substrates, chemically tailored for the method [57]. Thus, detection of cleavage was observed directly by mass spectroscopy without prior need for further purification of substrates and products. Compound DS-998 could also block the cleavage of MEK1 in HEK 293 cells [57]. Using the hydrazone bond of DS-998, Hanna *et al.* [58] generated a series of libraries, later analysed by *in vitro* assays in search for novel LFis. Many different inhibitors with significant differences in the types of inhibition were identified (compounds **71-73**, Table **8**). IC_{50} values were in the micromolar range with similar *K*is to the initial lead compound DS-998 [58].

10. Inhibitors Derived from Natural Products

Catechins from green tea inhibited LF metalloprotease activity with an IC_{50} of 0.1 μM [59]. One of them, epigallocatechin-3-gallate (ECGC) (compound **74**, Scheme **4**), completely prevented LF-induced macrophage toxicity at a concentration of 10 μM. The *in vivo* activity of ECGC was encouraging because it completely prevented LF-induced death of Fischer 344 rats when pre-incubated with the toxin simultanesously causing a consistent and long delay of animal death when administered independently of LF [59].

11. Compounds with Polyphenols Motifs

Ten commercially available compounds bearing a polyphenol motif were screened to identify four effective inhibitors against LF [60]. One of them (compound **75**, Scheme **4**; K_i 1.8 μM) was very potent under physiological salt concentrations providing an encouraging precedent for the further generation of a carbohydrate-based library of inhibitors. Synthesis of a library of tetrahydroisoquinolines by diversifying the 5- hydroxydopamine core using the Pictet-Spengler reaction and subsequent screening gave six hits. One of them (compound **76**, Scheme **4**) was a very potent non-competitive inhibitor and exhibited a K_i of 4.3 μM under physiological salt concentrations.

Table 7. Analogues of Compound 62

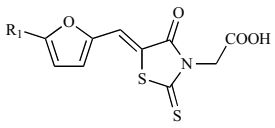

Compound	R_1	IC_{50} (nM)
63	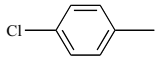	900
64	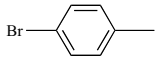	850
65	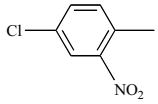	500
66	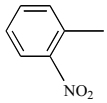	3100
67	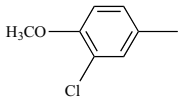	298
68	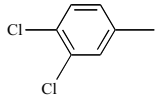	265
69	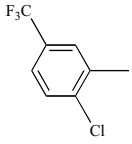	32 (K_i)

Table 8. Hydrazone Inhibitors of LF

Compound	Inhibitor	IC_{50} (μM)
70 (DS-998)	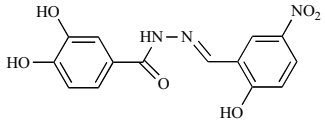	200
71	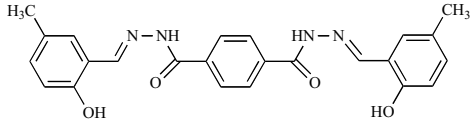	80
72	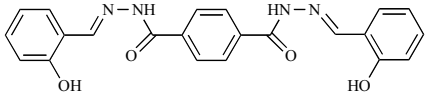	50
73	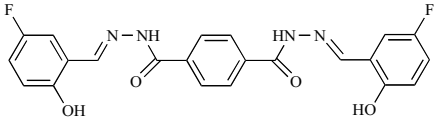	50

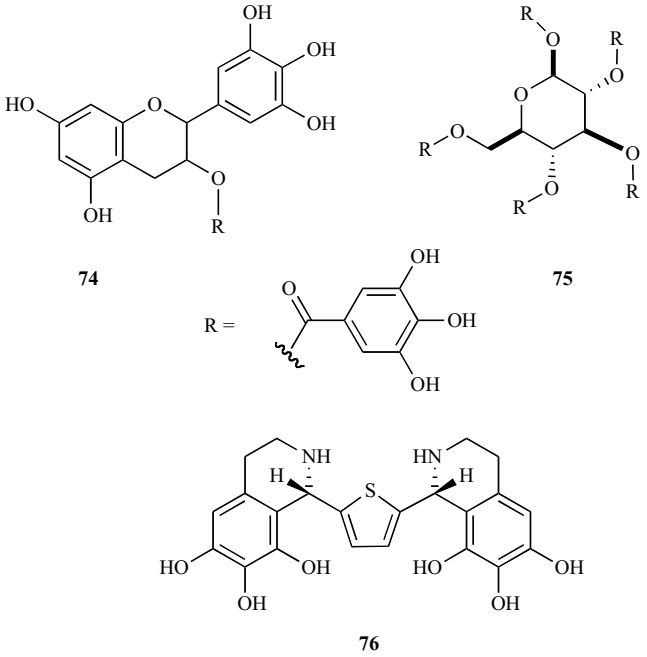

Scheme 4.

12. Phenylfuran, Phenylpyrazole, and Phenylpyrrole Carboxylic Derivatives

A chemical diversity library of 10,000 drug-like molecules was recently screened to identify novel LFis [61]. The library comprised a large collection of commonly accepted pharmaceutical hit compounds, including non-functionalized carboxylic acid derivatives, but excluding hydroxamate-, aminoglycoside-, tetracycline- and gallate-based scaffolds. High-throughput fluorescence microplate assays measuring *in vitro* LF activity, were utilized with an initial hit rate of 3.9%, that was further reduced by applying a series of experimental filters (solubility measurements, determination of nonspecific inhibition, dose-response relationship for enzyme inhibition). The most potent LFis with IC_{50} < 11 μM (Table **9**) were screened in more detail by an HPLC-based assay measuring LF activity to identify false positives.

Table 9. Phenylfuran, Phenylpyrazole, and Phenylpyrrole Carboxylic Derivatives

Compound	Chemical Structure	IC_{50} / K_i (μM)
77	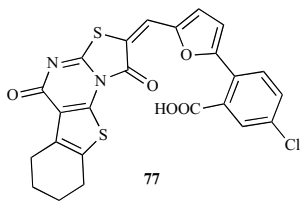 **77**	0.8 / 1.1
78	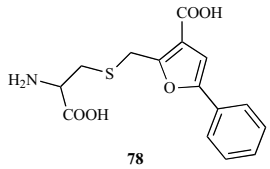 **78**	3.6 / 2.9
79	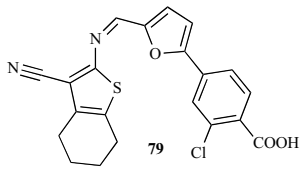 **79**	4.2 / 2.4

(Table 9. Contd….)

Compound	Chemical Structure	IC_{50} / K_i (μM)
80	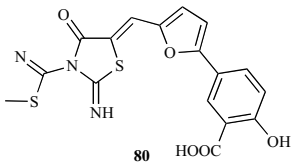 **80**	4.8 / 3.1
81	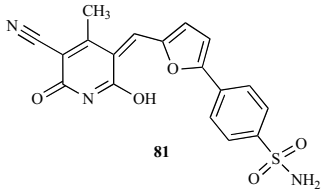 **81**	8.3 / 5.4
82	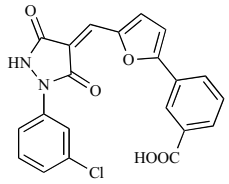 **82**	10.5 / 7.2
83	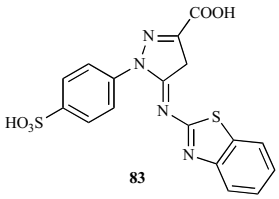 **83**	7.7 / 4.2
84	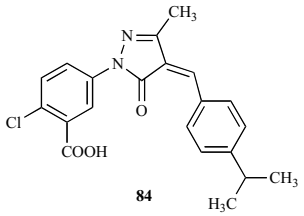 **84**	7.9 / 0.9
85	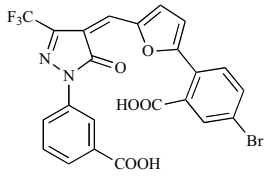 **85**	1.7 / 1.6
86	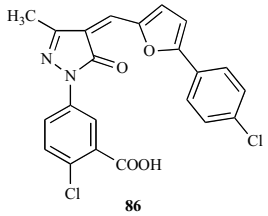 **86**	10.7 / 2.1

(Table 9. Contd….)

Compound	Chemical Structure	IC_{50} / K_i (μM)
87	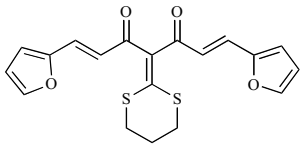 **87**	3.0 / 2.7
88	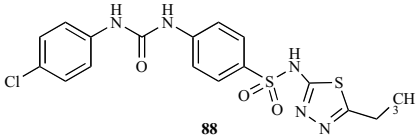 **88**	3.9 / 0.9
89	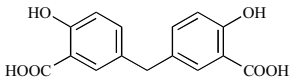 **89**	3.1 / 2.4
90	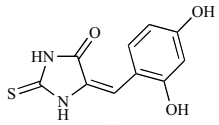 **90**	3.4 / 1.1
91	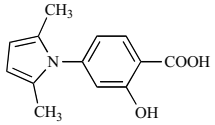 **91**	4.3 / 1.5
92	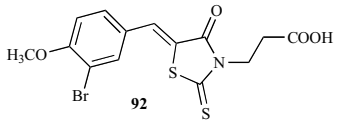 **92**	4.4 / 3.3
93	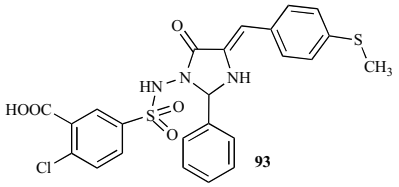 **93**	3.6 / 2.5
94	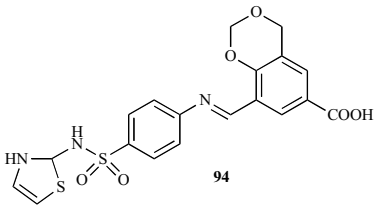 **94**	9.3 / 1.8

Kinetic studies of the finally selected 18 potent LFis exhibited mixed-mode competitive inhibition with *K*is in the range of 1–5 μM [61]. The 18 LFis were classified in two main groups: 2-phenylfurans (compounds **77**-**82**, Table **9**) and *N*-phenyl-dihydropyrazoles (compounds **83** and **84**). Compounds **85** and **86** possessed both fragments. A set of novel LFis contained in addition phenylimidazole, phenylpyrrole, and phenylpyrazolidine substructures (compounds **93**, **91**, and **82**, respectively), that were isosteric to the phenylfuran and phenyldihydropyrazole moieties. Molecular modeling studies revealed that some of the mentioned LFis could fit quite well with previously published pharmacophore models

[52]. Compounds **87** and **88** that contained 1,3-dithian-2-ylidene and *N*,*N*-diphenylurea-sulfonamide fragments respectively, represent a novel structural class of highly active LFis.

CONCLUDING REMARKS

Despite the potential use of Anthrax as biological weapon, there is no routine effective therapy for anthrax contacted by inhalation. It is envisaged that a microbial antibiotic combined with an LF-inhibitor could increase host survival. A low molecular weight inhibitor would be invaluable in combating the lethal toxin by reducing or preventing the damage to vascular circulation, giving the time for the antibiotics to neutralize the bacterial infection. A concentrated effort in anthrax toxin research has resulted in the design of potent inhibitors that can specifically interfere with the catalytic activity of LF. Inhibitors were identified by peptide and chemical library screens, coupled with structure-based computer modeling. The promising data obtained suggest that the design of new, even more potent bioactive compounds with specific inhibitory activity on LF protease is feasible.

NOTE

While this review was in press, two articles reporting new LF inhibitors were published. In the first one Pellecchia and co-workers [62] carried out a HTS against LF (ASDI library, 14.000 compounds), which yielded six bioactive compounds. Among them, there are two compounds contained a rhodanine moiety, which has been previously identified as an effective Zn^{2+} chelating scaffold, as well [55,56,61].

In the second one, Gaddis *et al.* [63] identified initially an LF binder by a medium throughput cell-based screen, which became a potent inhibitor through subsequent SAR studies. Mechanistic studies identified these agents as uncompetitive inhibitors of LF with K_i values of 3.0 and 1.7 μM, respectively, with good cell potency and low cytotoxicity.

ABBREVIATIONS

LF	=	Anthrax lethal factor
MAPKK	=	Mitogen-Activated Protein Kinase Kinase
B. anthracis	=	*Bacillus anthracis*
EF	=	Edema factor
PA	=	Protective antigen
ETx	=	Edema toxin
LTx	=	Lethal toxin
ATR	=	Anthrax toxin receptor
PA_{20}	=	N-terminal fragment of PA
PA_{63}	=	C-terminal fragment of PA
MEK	=	MAPK/ERK (Extracellular-signal-Regulated Kinase) Kinase
MKK	=	MAPK (Mitogen-Activated Protein Kinase) Kinase
LFi	=	Anthrax lethal factor inhibitor
MMPs	=	Matrix Metallo-Proteinases
MMPis	=	Matrix Metallo-Proteinases inhibitors
PDB	=	Protein Data Bank
QSAR	=	Qualitative Structure-Activity Relationship
IC_{50}	=	The half of maximal Inhibitory Concentration
CoMFA	=	Comparative Molecular Field Analysis (CoMFA)

REFERENCES

[1] Mock, M.; Fouet, A. *Annu. Rev. Microbiol.*, **2001**, *55*, 647.
[2] Dixon, T.C.; Meselson, M.; Guillemin J.; Hanna P.C. *N. Engl. J. Med.*, **1999**, *341*, 815.
[3] Hanna, P.C.; Ireland, J.A.W. *Trends Microbiol*., **1999**, *7*, 180.
[4] Cieslak, T.J.; Eitzen, E.M. *Emerg. Infect. Dis*., **1999**, *5*, 552.
[5] Hanna, P.C.; Acosta, D.; Collier, R.J. *Proc. Natl. Acad. Sci. U.S.A.*, **1993**, *90*, 10198.
[6] Dixon, T.C.; Fadl, A.A.; Koehler, T.M.; Swanson, J.A.; Hanna, P.C. *Cellular Microbiology*, **2000**, *2*, 453.
[7] Gill, D.M. In *Bacterial Toxins and Cell Membranes*, Jeljaszewica, J.; Wadstrom, T., Eds.; Academic Press, New York, **1978**; pp. 291-332.
[8] Uchida, I.; Hornung, J.M.; Thorne, C.B.; Klimpel, K.R.; Leppla, S.H. *J. Bacteriol*., **1993**, *175*, 5329.
[9] Dai, Z.; Sirard, J.C.; Mock, M.; Koehler, T.M. *Mol. Microbiol*., **1995**, *16*, 1171.
[10] Dai, Z.; Koehler, T.M. *Infect. Immun.*, **1997**, *65*, 2576.
[11] Mignot, T.; Mock, M.; Fouet, A. *Mol. Microbiol.*, **2003**, *47*, 917.
[12] Mock, M.; Fouet, A. *Curr. Opin. Microbiol*., **2006**, *9*, 160.
[13] Petosa, C.; Collier, R.J.; Klimpel, K.R.; Leppla, S.H.; Liddington, R.C. *Nature*, **1997**, *385*, 833.
[14] Bradley, K.A.; Mogridge, J.; Mourez, M.; Collier, R.J.; Young, J.A. *Nature*, **2001**, *414*, 225.
[15] Milne, J.C.; Furlong, D.; Hanna, P.C.; Wall, J.S.; Collier, R.J. *J. Biol. Chem*., **1994**, *269*, 20607.
[16] Mogridge, J.; Cunningham, K.; Collier, R.J. *Biochemistry*, **2002**, *41*, 1079.
[17] Baldari, C.T.; Tonello, F.; Paccani, S.R.; Montecucco, C. *Trends Immunol.*, **2006**, *27*, 434.
[18] Duesbery, N.S.; Webb, C.P.; Leppla, S.H.; Gordon, V.M.; Klimpel, K.R.; Copeland, T.D.; Ahn, N.G.; Oskarsson, M.K.; Fukasawa, K.; Paull, K.D.; Vande Woude, G.F. *Science*, **1998**, *280*, 734.
[19] Vitale, G.; Pellizzari, R.; Recchi, C.; Napolitani, G.; Mock, M.; Montecucco, C. *Biochem. Biophys. Res. Commun*., **1998**, *248*, 706.
[20] Park, J.M.; Greten, F.R.; Li, Z.W.; Karin, M. *Science*, **2002**, *297*, 2048.
[21] Bardwell, A.J.; Abdollahi, M.; Bardwell, L. *Biochem. J*., **2004**, *378*, 569.
[22] Vitale, G.; Bernardi, L.; Napolitani, G.; Mock, M.; Montecucco, C. *Biochem. J.*, **2000**, *352*, 739.
[23] Agrawal, A.; Lingappa, J.; Leppla, S.H.; Agrawal, S.; Jabbar, A.; Quinn, C.; Pulendran, B. *Nature*, **2003**, *424*, 329.
[24] Schechter, I.; Berger, A. *Biochem. Biophys. Res. Commun.*, **1967**, *27*, 157.
[25] Pannifer, A.D.; Wong, T.Y.; Schwarzenbacher, R.; Renatus, M.; Petosa, C.; Bienkowska, J.; Lacy, D.B.; Collier, R.J.; Park, S.; Leppla, S.H.; Hanna, P.; Liddington, R.C. *Nature*, **2001**, *414,* 229.
[26] Arora, N.; Leppla, S.H. *J. Biol. Chem*., **1993**, *268*, 3334.
[27] Humphrey, W.; Dalke, A.; Schulten, K. *J. Mol. Graph.,* **1996**, *14*, 33.
[28] Klimpel, K.R.; Arora, N.; Leppla, S.H. *Mol. Microbiol*., **1994**, *13*, 1093.
[29] Hammond, S.E.; Hanna, P.C. *Infect. Immun*., **1998**, *66*, 2374.
[30] Tonello, F.; Naletto, L.; Romanello, V.; Dal Molin, F.; Montecucco, C. *Biochem. Biophys. Res. Commun.*, **2004**, *313*, 496.
[31] Spyroulias, G.A.; Galanis, A.S.; Pairas, G.; Manessi-Zoupa, E.; Cordopatis, P. *Curr. Top. Med. Chem*., **2004**, *4*, 403.
[32] Pezard, C.; Berche, P.; Mock, M. *Infect. Immun*., **1991**, *59*, 3472.

[33] Tonello, F.; Seveso, M.; Marin, O.; Mock, M.; Montecucco, C. *Nature*, **2002**, *418*, 386.
[34] Cummings, R.T.; Salowe, S.P.; Cunningham, B.R.; Wiltsie, J.; Park, Y.W.; Sonatore, L.M.; Wisniewski, D.; Douglas, C.M.; Hermes, J.D.; Scolnick, E.M. *Proc. Natl Acad. Sci. U.S.A.*, **2002**, *99*, 6603.
[35] Turk, B.E.; Wong, T.Y.; Schwarzenbacher, R.; Jarrell, E.T.; Leppla, S.H.; Collier, R.J.; Liddington, R.C.; Cantley, L.C. *Nat. Struct. Mol. Biol.*, **2004**, *11*, 60.
[36] Gowravaram, M.R.; Tomczuk, B.E.; Johnson, J.S.; Delecki, D.; Cook, E.R.; Ghose, A.K.; Mathiowetz, A.M.; Spurlino, J.C.; Rubin, B.; Smith, D.L.; Pulvino, T.; Wahl, R.C. *J. Med. Chem*., **1995**, *38*, 2570.
[37] Baxter, A.D.; Bird, J.; Bhogal, R.; Massil, T.; Minton, K.J.; Montana, J.; Owen, D.A. *Bioorg. Med. Chem. Lett*., **1997**, *7*, 897.
[38] Grobelny, D.; Poncz, L.; Galardy, R.E. *Biochemistry*, **1992**, *31*, 7152.
[39] Lindsey, M.L. *Mini Rev. Med. Chem*., **2006**, *6*, 1243.
[40] Turk, B. *Nat. Rev. Drug Disc*., **2006**, *5*, 785.
[41] Whittaker M.; Floyd, C.D.; Brown, P.; Andrew J. H. *Chem. Rev*., **1999**, *99*, 2735.
[42] Kocer, S.S.; Walker, S.G.; Zerler, B.; Golub, L.M.; Simon, S.R. *Infect. Immun.*, **2005**, *73*, 7548.
[43] Xiong, Y.S.; Wiltsie, J.; Woods, A.; Guo, J.; Pivnichny, J.V.; Tang, W.; Bansal, A.; Cummings, R.T.; Cunningham, B.R.; Friedlander, A.M.; Douglas, C.M.; Salowe, S.P.; Zaller, D.M.; Scolnick, E.M.; Schmatz, D.M.; Bartizal, K.; Hermes, J.D.; MacCoss, M.; Chapman, K.T. *Bioorg. Med. Chem. Lett*., **2006**, *16*, 964.
[44] Shoop, W.L.; Xiong, Y.; Wiltsie, J.; Woods, A.; Guo, J.; Pivnichny, J.V.; Felcetto, T.; Michael, B.F.; Bansal, A.; Cummings, R.T.; Cunningham, B.R.; Friedlander, A.M.; Douglas, C.M.; Patel, S.B.; Wisniewski, D.; Scapin, G.; Salowe, S.P.; Zaller, D.M.; Chapman, K.T.; Scolnick, E.M.; Schmatz, D.M.; Bartizal, K.; MacCoss, M. *Proc. Natl. Acad. Sci. U.S.A*., **2005**, *102*, 7958.
[45] Lee, L. V.; Bower, K.E.; Liang, F.-S.; Shi, J.; Wu, D.; Sucheck, S.J.; Vogt, P.K.; Wong, C.-H. *J. Am. Chem. Soc*., **2004**, *126*, 4774.
[46] Fridman, M.; Belakhov, V.; Lee, L.V.; Liang, F.-S.; Wong, C.-H.; Baasov, T. *Angew. Chem. Int. Ed. Engl.,* **2005**, *44*, 447.
[47] Fridman, M.; Belakhov, V.; Yaron, S.; Baasov, T. *Org. Lett*., **2003**, *5*, 3575.
[48] Ren, Y.G.; Martinez, J.; Kirsebom, L.A.; Virtanen, A. *RNA*, **2002**, *8*, 1393.
[49] Jiao, G.S.; Cregar, L.; Goldman, M.E.; Millis, S.Z.; Tang, C. *Bioorg. Med. Chem. Lett*., **2006**, *16*, 1527.
[50] Jiao, G.S.; Simo, O.; Nagata, M.; O'Malley, S.; Hemscheidt, T.; Cregar, L.; Millis, S.Z.; Goldman, M.E.; Tang, C. *Bioorg. Med. Chem. Lett*., **2006**, *16*, 5183.
[51] Goldman M.E.; Cregar, L.; Nguyen, D.; Simo, O.; O'Malley, S.; Humphreys, T. *BMC Pharmacol.*, **2006**, *6*, 8.
[52] Panchal, R.G.; Hermone, A.R.; Nguyen, T.L.; Wong, T.Y.; Schwarzenbacher, R.; Schmidt, J.; Lane, D.; McGrath, C.; Turk, B.E.; Burnett, J.; Aman, M.J.; Little, S.; Sausville, E.A.; Zaharevitz, D.W.; Cantley, L.C.; Liddington, R.C.; Gussio, R.; Bavari, S. *Nat. Struct. Mol. Biol.*, **2004**, *11*, 67.
[53] Montecucco, C.; Tonello, F.; Zanotti, G. *Trends Biochem. Sci.*, **2004**, *29*, 282.
[54] Lewis, J.A.; Mongan, J.; McCammon, J.A.; Cohen, S.M. *ChemMedChem*, **2006**, *1*, 694.
[55] Forino, M.; Johnson, S.; Wong, T.Y.; Rozanov, D.V.; Savinov, A.Y.; Li, W.; Fattorusso, R.; Becattini, B.; Orry, A.J.; Jung, D.; Abagyan, R.A.; Smith, J.W.; Alibek, K.; Liddington, R.C.; Strongin, A.Y.; Pellecchia, M. *Proc. Natl. Acad. Sci. U.S.A*., **2005**, *102*, 9499.
[56] Johnson, S.L.; Jung, D.; Forino, M.; Chen, Y.; Satterthwait, A.; Rozanov, D.V.; Strongin, A.Y.; Pellecchia, M. *J. Med. Chem*., **2006**, *49*, 27.
[57] Min, D.H.; Tang, W.J.; Mrksich, M. *Nature Biotechnol*., **2004**, *22*, 717.
[58] Hanna, M.L.; Tarasow, T.M.; Perkins, J. *Bioorg. Chem*., **2007**, *35*, 50.
[59] Dell'Aica, I.; Dona, M.; Tonello, F.; Piris, A.; Mock, M.; Montecucco, C.; Garbisa, S. *EMBO Rep*., **2004**, *5*, 418.
[60] Numa, M.M.; Lee, L.V.; Hsu, C.C.; Bower, K.E.; Wong, C.H. *ChemBioChem*, **2005**, *6*, 1002.
[61] Schepetkin, I.A.; Khlebnikov, A.I.; Kirpotina, L.N.; Quinn, M.T. *J. Med. Chem*., **2006**, *49*, 5232.
[62] Johnson, S.L.; Chen, L.-H.; Pellecchia, M. *Bioorg. Chem*., **2007**, *35*, 306.
[63] Gaddis, B.D; Avramova, L.V; Chmielewski, J. *Bioorg. Med. Chem. Lett.*, **2007**, *17*, 4575.

Received: 21 February, 2007 Revised: 04 December, 2007 Accepted: 05 December, 2007